Int. J. Electrochem. Sci., 9 **(2014)** 3078 - 3086

International Journal of
ELECTROCHEMICAL
SCIENCE
www.electrochemsci.org

Effect of the Substitution of Co by $V_{0.81}Fe_{0.19}$ on Phase Structure and Electrochemical Characteristics of $La_{0.7}Ce_{0.7}Ni_{3.6}Co_{0.7-x}Al_{0.35}Mn_{0.35}(V_{0.81}Fe_{0.19})_x$ Alloys

Xianguang Shang[1], *Shan Lu*[2], *Zhiyuan Zhang*[3], *Yanping Fan*[1,*], *Baozhong Liu*

[1] School of Physics and Chemistry, Henan Polytechnic University, Jiaozuo 454000, China
[2] Department of Mechanic and Electrical Engineering, Jiaozuo University, Jiaozuo 454000, China
[3] Inner Mongolia Rare Earth Ovonic Metal Hydride Co. Ltd., Baotou 014030, China
[*]E-mail: hpuforrest@126.com

Received: 10 January 2014 / *Accepted:* 27 February 2014 / *Published:* 23 March 2014

Herein, phase structure and electrochemical performances of $La_{0.7}Ce_{0.7}Ni_{3.6}Co_{0.7-x}Al_{0.35}Mn_{0.35}(V_{0.81}Fe_{0.19})_x$ hydrogen storage alloys were investigated. X-ray diffraction results indicate that all alloys are $LaNi_5$ phase with $CaCu_5$ structure, and lattice parameter *a*, *c* and cell volume *V* increase with increasing *x* value. The activation property of the alloy electrodes is improved by increasing $V_{0.81}Fe_{0.19}$ content. Maximum discharge capacity of the alloy electrodes decreases from 351.5 mAh/g (*x* = 0) to 343.2 mAh/g (*x* = 0.20) with increasing *x* value. The high-rate dischargeability at the discharge current density of 1200 mA/g of the alloy electrodes first increases from 58.5% (*x* = 0) to 75.5% (*x* = 0.10), and then decreases to 66.7 (*x* = 0.20) when *x* increases to 0.20. Cycling capacity retention rate decreases with increasing *x* value, which is ascribed to the degradation of corrosion resistance of the alloy electrodes.

Keywords: Hydrogen storage alloy; Phase structure; Electrochemical property; Kinetics

1. INTRODUCTION

AB_5-type alloys have attracted much attention due to their widespread applications in rechargeable nickel/metal hydride (Ni/MH) batteries [1]. In order to broaden application field of Ni/MH batteries and enhance their competition abilities, a realistic approach is to reduce the cost of AB_5-type alloy [2]. The cost of cobalt is the highest among raw material of AB_5-type alloy, and many attempts have been made to decrease the cost of alloy by substituting Co with foreign metals, such as, Fe, Cu, Si etc, whose raw cost was much cheaper compared with Co [3-5]. However, the performance-

price ratio of the alloy electrodes is yet unsatisfactory. Consequently it is necessary to improve the electrochemical properties with reducing the raw cost of AB_5-type alloy.

Li et al. reported that the addition of V in $Mm(NiCoMnAlV)_5$ alloy also improved the discharge capacity and kinetic properties [6]. The discharge capacity and activation of $LaNi_{3.6}Al_{0.4}Co_{0.7}Mn_{0.3}V_y$ alloys can be improved by adding V if y is 0.02-0.1, and high-rate dischargeability was also enhanced due to the increase in kinetic performance [7,8]. Obviously the addition of V element is effective to enhance the activation performance and the high-rate dischargeability. However, the price of pure V is very high and is similar to that of Co. Fortunately, the price of commercial $V_{0.81}Fe_{0.19}$ alloy is 90% less than that of pure V. Furthermore, the Fe addition in AB_5 alloy can obviously modify the cycling stability due to the improvement of pulverization resistance[9,10]. In addition, in our previous investigations [11-13], it has been proven that $V_{0.81}Fe_{0.19}$ is successfully used as additive instead of pure V in AB_5 type alloys. Thus, it is feasible and promising to substitute Co using $V_{0.81}Fe_{0.19}$ rather than pure V in AB5 type hydrogen storage alloy.

Here, on the basis of the merits of $V_{0.81}Fe_{0.19}$ and the belief that the substitution of Co by $V_{0.81}Fe_{0.19}$ may result in some noticeable modification of hydrogen storage properties, microstructures and electrochemical hydrogen storage properties of $La_{0.7}Ce_{0.7}Ni_{3.6}Co_{0.7-x}Al_{0.35}Mn_{0.35}(V_{0.81}Fe_{0.19})_x$ (x = 0-0.3) alloys have been investigated systematically.

2. EXPERIMENTAL PROCEDURES

$La_{0.7}Ce_{0.7}Ni_{3.6}Co_{0.7-x}Al_{0.35}Mn_{0.35}(V_{0.81}Fe_{0.19})_x$ (x = 0-0.3) alloys were synthesized by induction melting of the metal elements (La, Ce, Ni, Mn, Cu: 99.9% purity and commercial VFe alloy contained 81.0 at.% V and the other were Fe and trace impurities.) in argon atmosphere and then were annealed at 1223 K for 10 h under in atmosphere with the pressure of 0.08 MPa.

The phases of the alloy powders were determined by X-ray diffraction (XRD) using a Rigaku D/max 2500PC powder diffractometer with Cu Kα radiation. The phase structures of the alloys were analyzed using Jade-5 software.

All the alloy electrodes for test were prepared by cold pressing the mixture of 0.15 g alloy powders of 200-400 meshes and 0.75 g nickel carbonyl powders into a pellet of 10 mm in diameter under 15 MPa. Electrochemical measurements were performed at 298 K in a standard tri-electrode system, consisting of a working electrode (metal hydride), a counter electrode ($Ni(OH)_2$/NiOOH), and a reference electrode (Hg/HgO) with 6mol/L KOH solution as electrolyte. Each electrode was charged for 7 h at 60 mA/g and discharged to -0.6 V versus Hg/HgO at 60 mA/g at 298 K. After every charging/discharging, the rest time was 10 min. In evaluating the high-rate dischargeability, discharge capacity of the alloy electrode at different discharge current density were measured. The high-rate dischargeability HRD (%) was defined as $C_d/C_{max} \times 100\%$, where C_d was the discharge capacity at the discharge current density I_d (I_d = 60, 300, 600, 900 and1200 mA/g) and C_{max} was the maximum discharge capacity at the discharge current density I_d = 60 mA/g.

The linear polarization curve and potential-step measurement were obtained by Advanced Potentiostat/Galvanostat (PARSTAT 2273), respectively. At 50% depth of discharge (DOD), the linear

polarization curve was obtained by scanning the electrodes from -5 to 5 mV (vs. open circuit potential). For potential-step measurement, the electrodes in fully charged state were discharged with potential steps of 0.5 V for 3600 s.

3. RESULTS AND DISCUSSION

3.1 Crystal structure

Fig. 1 presents XRD patterns of $La_{0.7}Ce_{0.7}Ni_{3.6}Co_{0.7-x}Al_{0.35}Mn_{0.35}(V_{0.81}Fe_{0.19})_x$ alloys. It can be seen that all alloys are $LaNi_5$ phase with $CaCu_5$ structure. Calculated lattice parameters of $LaNi_5$ phase in all alloys are listed in Table 1. It can be seen that lattice parameter *a*, *c* and cell volume *V* of $LaNi_5$ phase increase with the increase of *x* value, which may be ascribed to larger atomic radius of Fe (1.72 Å) and V (1.92 Å) compared with Co (1.67 Å).

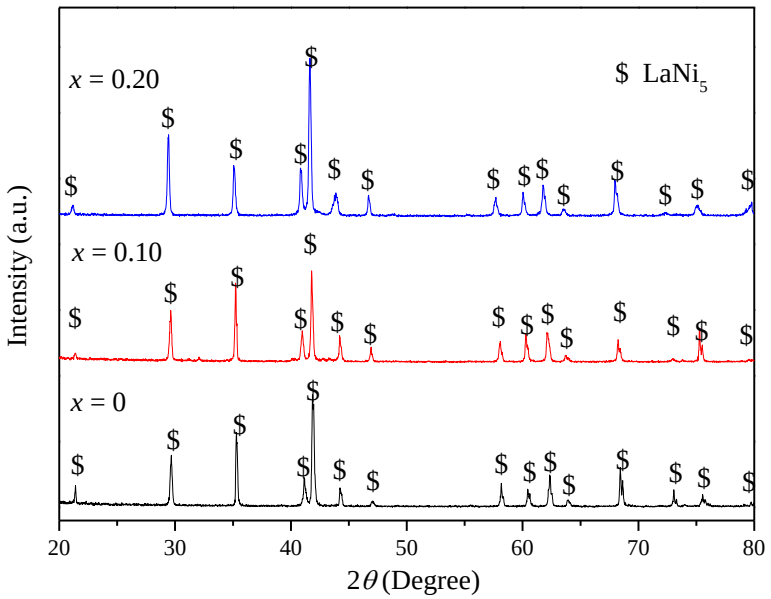

Figure 1. XRD patterns of $La_{0.7}Ce_{0.7}Ni_{3.6}Co_{0.7-x}Al_{0.35}Mn_{0.35}(V_{0.81}Fe_{0.19})_x$ alloys

Table 1. Lattice parameters of $La_{0.7}Ce_{0.7}Ni_{3.6}Co_{0.7-x}Al_{0.35}Mn_{0.35}(V_{0.81}Fe_{0.19})_x$ alloys

x	*a*/Å	*c*/Å	*V*/Å^3
0	5.0839	4.0575	90.82
0.10	5.1112	4.0581	91.81
0.20	5.1531	4.0604	93.37

3.2 Activation property and maximum discharge capability

The number of cycles (N_a) needed to activate the electrodes and maximum discharge capacity

(C_{max}) of $La_{0.7}Ce_{0.7}Ni_{3.6}Co_{0.7-x}Al_{0.35}Mn_{0.35}(V_{0.81}Fe_{0.19})_x$ alloy electrodes are given in Table 2. The N_a decreases with increasing x value, indicating the substitution of Co by $V_{0.81}Fe_{0.19}$ improves the activation performance of the alloy electrodes. The V-dissolution makes the electrode surface of the alloys containing V change to microporous surface, which is very helpful to hydrogen penetration so that the fast initial activation occurs [6]. The increase in V content is beneficial to the activation property of the alloy electrodes. However, Wu et al. [14] reported the oxidation film formed on the surface of the electrode alloy increased the additive internal energy, which led to the poorer activation performance. Due to the low surface energy of Fe, the increase in Fe makes the surface oxide layer become thick and leads to the increase in internal energy, and then degrades activation property. Thus, the activation performance of the alloy electrodes is mainly ascribed to the synthesized effect of V and Fe. The C_{max} of $La_{0.7}Ce_{0.7}Ni_{3.6}Co_{0.7-x}Al_{0.35}Mn_{0.35}(V_{0.81}Fe_{0.19})_x$ alloy electrodes decreases with increasing x value. In general, maximum discharge capacity is related to the crystalline structure and electrochemical kinetics (charge-transfer reaction and hydrogen diffusion). The addition of V in the AB_5 alloy contributed to the increase of discharge capacity [8]. The increase of V with increasing x value is beneficial to the maximum discharge capacity. Moreover, Li et al. [6] reported that the charge-transfer reaction can be speeded up by adding V in the AB_5-type alloy, which contributed to the charge-transfer reaction on the alloy surface. The increase in V content with increasing x value causes the improvement in charge-transfer reaction, which is beneficial to the discharge capacity. Unfortunately, the increase in Fe content with increasing x value makes the surface oxide layer become thick, which degrades the charge-transfer reaction on the alloy surface and makes the hydrogen diffuse from inner of the bulk electrode to the surface more difficultly. The decrease in electrochemical kinetics due to Fe introduction is unfavorable to the discharge capacity. It is reasonable to believe that disadvantageous factors are prominent for the decrement of the C_{max} of alloy electrodes in present work.

Table 2. Electrochemical properties of $La_{0.7}Ce_{0.7}Ni_{3.6}Co_{0.7-x}Al_{0.35}Mn_{0.35}(V_{0.81}Fe_{0.19})_x$ alloy electrodes

x	C_{max} (mAh/g)	N_a[b]	HRD_{1200}[a] (%)	S_{100} (%)
0	351.5	4	58.8	87.5
0.10	345.4	3	75.5	84.2
0.20	343.2	2	66.7	83.1

[a] The high-rate dischargeability at the discharge current density of 1200 mA/g.

[b] The number of cycles needed to activate the electrode.

3.3 High-rate dischargeability and electrochemical kinetics

Fig. 2 shows the relationship between the high-rate dischargeability (HRD) and discharge current density of $La_{0.7}Ce_{0.7}Ni_{3.6}Co_{0.7-x}Al_{0.35}Mn_{0.35}(V_{0.81}Fe_{0.19})_x$ alloy electrodes. The HRD of the alloy electrodes first increases with increasing x from 0 to 0.1, and then decreases when x increases to 0.3.

The HRD at the discharge current density of 1200 mA/g (HRD_{1200}) is listed in Table 2. It can be seen that HRD_{1200} first increases from 58.8% (x = 0) to 75.5% (x = 0.1), and then decreases to 66.7% (x = 0.3).

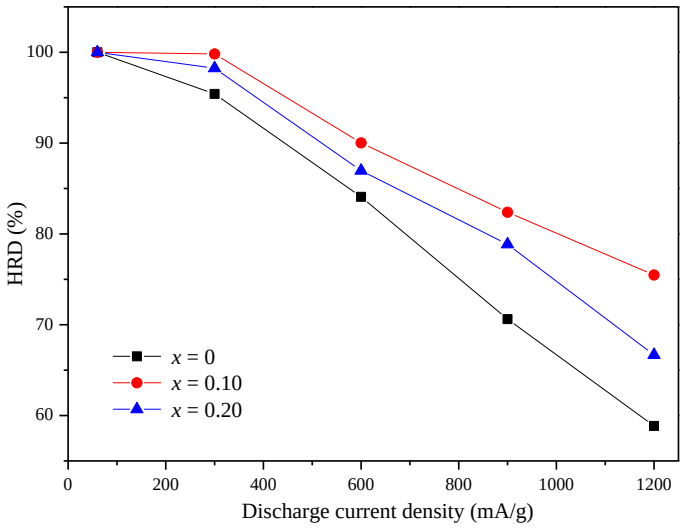

Figure 2. HRD of $La_{0.7}Ce_{0.7}Ni_{3.6}Co_{0.7-x}Al_{0.35}Mn_{0.35}(V_{0.81}Fe_{0.19})_x$ alloy electrodes

It is well known that the HRD of the metal-hydride electrodes is dominated by the charge-transfer reaction at the electrode/electrolyte interface and the hydrogen diffusion rate within the bulky alloy electrode, which are reflected in the value of surface exchange current density (I_0), being a measure of the catalytic activity of an alloy, as well as in the hydrogen diffusion coefficient (D), which characterizes the mass transport properties of an alloy electrode [15].

Fig. 3 shows the linear polarization curves of $La_{0.7}Ce_{0.7}Ni_{3.6}Co_{0.7-x}Al_{0.35}Mn_{0.35}(V_{0.81}Fe_{0.19})_x$ alloy electrodes at 50% DOD and 298 K. The polarization resistances (R_p) is calculated through estimating the slopes of linear polarization curves, and listed in Table 3. The R_p values of the alloy electrodes first decreases from 184.6 mA/g (x = 0) to 165.9 mA/g (x = 0.1), and then increases to 208.9 mA/g (x = 0.3). The I_0 value can be calculated according to the following formula [16].

$$I_0 = \frac{RT}{FR_p} \qquad (1)$$

where R, T, F, R_p are the gas constant, absolute temperature, Faraday constant and the polarization resistance, respectively. The I_0 values are calculated by Eq. (1) and listed in Table 3. It is clear that the I_0 first increases from 139.1 mA/g (x = 0) to 154.8 mA/g (x = 0.1), and then decreases to 122.9 mA/g (x = 0.3). As mentioned above, the increase in V content improves the charge-transfer reaction on the surface of the alloy electrodes with increasing x value. On the other hand, Co contributes to the charge-transfer reaction at the electrode/electrolyte interface due to excellent electrocatalytic activity. the increase of Fe and decrease of Co will cause the increase of surface oxide film and then degrade the charge-transfer reaction on the alloy surface.

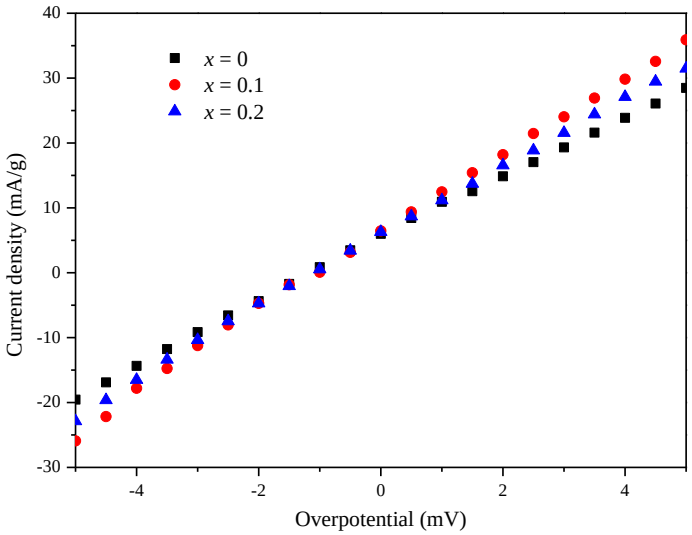

Figure 3. Linear polarization of $La_{0.7}Ce_{0.7}Ni_{3.6}Co_{0.7-x}Al_{0.35}Mn_{0.35}(V_{0.81}Fe_{0.19})_x$ alloy electrodes

Fig. 4 shows the semi-logarithmic plots of the anodic current vs. the time response of $La_{0.7}Ce_{0.3}Ni_{4.2}Mn_{0.9-x}Cu_{0.37}(V_{0.81}Fe_{0.19})_x$ alloy electrodes. Zheng et al. [17] reported that in a large anodic potential-step test, after a long discharge time, the diffusion current varies with time according to the following equation:

$$\lg i = \lg(\frac{6FD}{da^2}(C_0 - C_s) - \frac{\pi^2}{2.303}\frac{D}{a^2}t \qquad (2)$$

where i is anodic current density (A/g), D the hydrogen diffusion coefficient (cm^2/s), d the density of the alloy (g/cm^3), a the radius of the alloy particle, C_0 the initial hydrogen concentration in the bulk of the alloy (mol/cm^3), C_s the surface hydrogen concentration of the alloy (mol/cm^3) and t is the discharge time (s). Assuming that the alloy powders have a similar particle distribution with an average particle radius of 13 μm, the D is calculated and summarized in Table 3. The D of $La_{0.7}Ce_{0.7}Ni_{3.6}Co_{0.7-x}Al_{0.35}Mn_{0.35}(V_{0.81}Fe_{0.19})_x$ alloy electrodes first increases from 7.72×10^{-11} (x = 0) to 8.89×10^{-11} cm^2/s (x = 0.1), and then decreases to 6.84×10^{-11} cm^2/s (x = 0.3). Wang et al. [18] reported that the process of dissolved element V in the bulk into the electrolyte forms a 'path' and the diameter of formed 'path' is a little larger than hydrogen atom. This microporous surface caused by the V-dissolution is very helpful to hydrogen penetration [8]. The increase in V content will contribute to the improvement in hydrogen diffusion with increasing x value. On the contrary, Iwakura et al. [19] have reported that the oxidation of Fe on the alloy surface limited the hydrogen transfer from the bulk to the surface, which is detrimental to the hydrogen diffusion. As mentioned above, the increase of Fe content causes the increase of surface oxide film, which will degrade the hydrogen diffusion. Moreover, metalic Co on the alloy surface made the hydrogen diffuse from the bulk to the surface more easily due to the good electrocatalytic activity and electrical conductivity. The decrease of Co content is unfavorable to the hydrogen diffusion property.

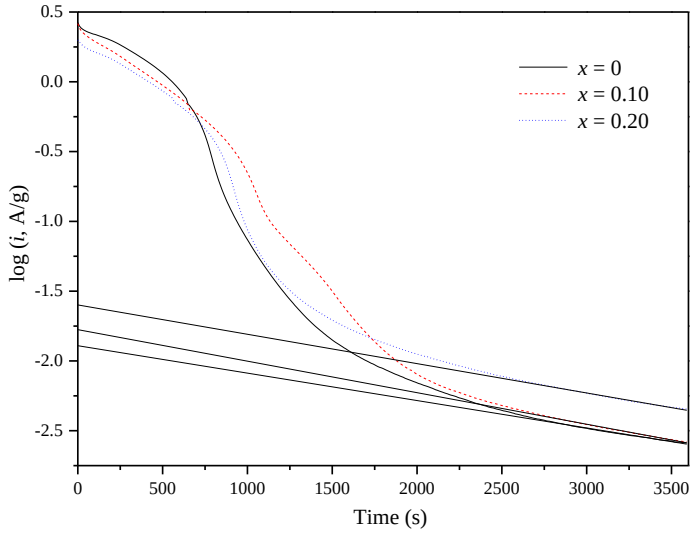

Figure 4. Semilogarithmic curves of anodic current vs. time of response of $La_{0.7}Ce_{0.7}Ni_{3.6}Co_{0.7-x}Al_{0.35}Mn_{0.35}(V_{0.81}Fe_{0.19})_x$ alloy electrodes

3.4 Cycling stability

The cycle stability is an extremely important factor for the service life of hydrogen storage alloys. The cycling capacity retention rate is expressed as $S_n(\%) = C_n/C_{max} \times 100$ (where C_n is the discharge capacity at the n^{th} cycle). The cycling capacity retention of $La_{0.7}Ce_{0.7}Ni_{3.6}Co_{0.7-x}Al_{0.35}Mn_{0.35}(V_{0.81}Fe_{0.19})_x$ alloy electrode as a function of cycle number is shown in Fig. 5. Cycling stability decreases with increasing x from 0 to 0.3. The S_{100} is listed in Table 2. It can be seen that S_{100} decreases from 91.2% (x = 0) to 84.8% (x = 0.3). Generally, the capacity decay of the alloy electrode is ascribed to the pulverization and corrosion [20], as well as to the decrease of the electrochemical kinetics at the surface [21]. The pulverization of the hydrogen storage alloy is induced by the strain based on the lattice expansion in the charge process. Liu et al. [22] pointed out that the larger the unit cell volume is, the interstitial hole size for hydrogen atoms to occupy is larger, the strain energy that hydrogen atoms to go in and out the crystal is smaller. The V of $LaNi_5$ matrix phase increases with increasing x value, which lowers the strain energy and then strengthens anti-pulverization property of the alloy electrodes. Unfortunately, V dissolves easily in the KOH, which leads to the loss of discharge capacity. The increase in V content is unfavorable for the cycling stability of the alloy electrodes with increasing x value. Meanwhile, Fe easily oxidized due to the lower surface energy, and coarse oxide film easily forms. Thus, it is believe that the decrease in corrosion resistance of alloy electrode is prominent for the degradation of cycling stability in present work.

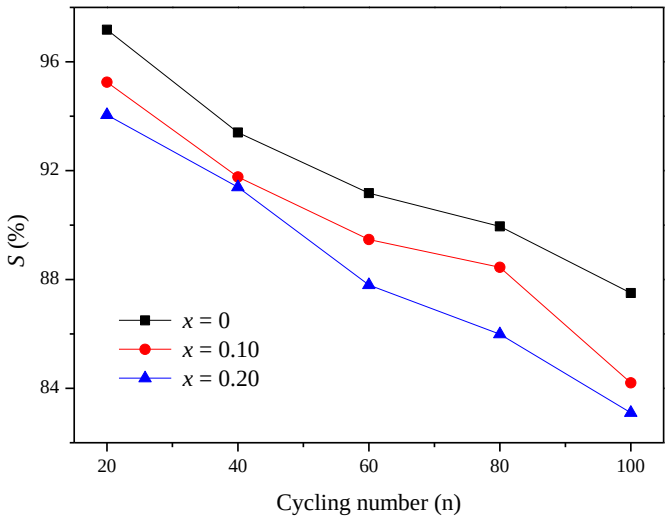

Figure 5. Cycling stability of $La_{0.7}Ce_{0.7}Ni_{3.6}Co_{0.7-x}Al_{0.35}Mn_{0.35}(V_{0.81}Fe_{0.19})_x$ alloy electrodes

4. CONCLUSIONS

Microstructures and electrochemical characteristics of $La_{0.7}Ce_{0.7}Ni_{3.6}Co_{0.7-x}Al_{0.35}Mn_{0.35}(V_{0.81}Fe_{0.19})_x$ hydrogen storage alloys were investigated. XRD results indicate that all alloys are $LaNi_5$ phase with $CaCu_5$ structure, and lattice parameter *a*, *c* and cell volume *V* increase with increasing *x* value. The activation property of the alloy electrodes is improved by increasing $V_{0.81}Fe_{0.19}$ content. Maximum discharge capacity of the alloy electrodes decreases with increasing *x* value. The HRD of the alloy electrodes first increases with increasing *x* from 0 to 0.10, and then decreases when *x* increases to 0.20. S_{100} decreases from 87.5% (*x* = 0.00) to 83.1% (*x* = 0.20), which is ascribed to the decrease of corrosion resistance of the alloy electrodes.

ACKNOWLEDGEMENTS
This research is financially supported by Program for Innovative Research Team (in Science and Technology) in the University of Henan Province (No. 2012IRTSTHN007) and the Doctoral Foundation of Henan Polytechnic University (B2010-13).

References

1. T. Sakai, H. Yoshinaga, H. Migamura, N. Kurigama, H. Ishikawa, *J. Alloys Compd.*, 180 (1992) 37
2. H. Ye, Y.X. Huang, J.X. Chen, H. Zhang, *J. Power Sources*, 103 (2002) 293
3. S. Yang, S. Han, J. Song, Y. Li, *J. Rare Earth*, 29 (2011) 692
4. M. Latroche, A. Percheron-Guegan, *J. Alloys Compd.*, 356 (2003) 461
5. X.B. Zhang, D.Z. Sun, W.Y. Yin, Y.J. Chai, M.S. Zhao, *Electrochim. Acta*, 50 (2005) 3407
6. R. Li, J.M Wu, H. Su, S.X. Zhou, *J. Alloys Compd.*, 421 (2006) 258
7. C.Y. Seo , S.J. Choi, J. Choi, C.N. Park, J.Y. Lee, *Int. J. Hydrogen Energy*, 28 (2003) 967
8. C.Y. Seo , S.J. Choi, J. Choi, C.N. Park, J.Y. Lee, *J. Alloys Compd.*, 351 (2003) 255

9. C. Iwakura, K. Ohkawa, H. Senoh, H. Inoue, *Electrochim. Acta*, 46 (2001) 4383
10. X.D. Wei, S.S. Liu, H. Dong, P. Zhang, Y.N. Liu, J.W. Zhu, G. Yu, *Electrochim. Acta*, 52 (2007) 2423
11. B.Z. Liu, M.J. Hu, Y. Zhou, A.M. Li, L.Q. Ji, Y.P. Fan, Z. Zhang, *J. Alloys Compd.*, 544 (2012) 105
12. B.Z. Liu, M.J. Hu, A.M. Li, L.Q. Ji, B.Q. Zhang, X.L. Zhu, *J. Rare Earths*, 30 (2012) 769
13. B.Z. Liu, X.Y. Peng, Y.P. Fan, L.Q. Ji, B.Q. Zhang, Z. Zhang, *Int. J. Electrochem. Sci.*, 7 (2012) 11966
14. M.S. Wu, H.R. Wu, Y.Y. Wang, C.C. Wan, *J. Alloys Compd.*, 302 (2000) 248
15. X.B. Zhang, D.Z. Sun, W.Y. Yin, Y.J. Chai, M.S. Zhao, *Chem. Phys. Phys. Chem.*, 6 (2005) 520
16. P. Notten, P. Hokkeling, *J. Electrochem. Soc.*, 138 (1991) 1877
17. G. Zheng, B.N. Popov, R.E. White, *J. Electrochem. Soc.*, 142 (1995) 2695
18. N. Wang, Y. Cai, *Rare Metal Materials and Engineering*, 40 (2011) 1519
19. C. Iwakura, M. Miyamoto, H. Inoue, M. Matsuoka, Y. Fukumoto, *J. Alloys Compd.*, 259 (1997) 132
20. D. Chartouni, F. Meli, A. Zuttel, K. Gross, L. Schlapbach, *J. Alloys Compd.*, 241 (1996) 160
21. B.Z. Liu, G.X. Fan, Y.C. Wang, G.F. Mi, Y.M. Wu, L.M. Wang, *Int. J. Hydrogen Energy*, 33 (2008) 5801
22. F.J. Liu, S. Suda, *J. Alloys Compd.*, 232 (1996) 204